



Capturing cold-formed steel shear wall behavior through nonlinear fastener-based modeling

Fani Derveni¹, Simos Gerasimidis², Kara D. Peterman³

Abstract

During the last few decades, cold-formed steel (CFS) has increasingly been used in low- and mid-rise construction across United States. Due to its high strength-to-weight ratio, its cost-efficiency, its ease in transportation and prefabrication, cold-formed steel as a structural or a non-structural component is commonly used as studs and tracks, joists, ledgers and as the main structural frame of shear walls in light-gauge construction. Cold-formed steel framed shear walls represent the principle lateral force resisting system. This work is focused on the stability of sheathed cold-formed steel framed shear walls subjected to lateral loads, such as earthquake and wind events, using the high fidelity finite element software ABAQUS. In particular, a fastener-based three-dimensional cold-formed steel shear wall model is simulated through nonlinear connector elements for steel-to-sheathing connections, orthotropic oriented strand board (OSB) as sheathing material at the exterior side and linear hold downs at the base of the wall for preventing uplift. This study aims to introduce a robust high fidelity finite element computational model, capable of accurately capturing the stability of wood sheathed cold-formed steel framed shear walls under lateral loading with potential use in a full building finite element simulation. Finally, the introduced model is validated by comparing the results with a recent experimental study, assessing the efficiency of numerical fastener-based models.

1. Introduction

Cold-formed steel (CFS) framed buildings are widely used for low- and mid-rise construction in United States. During the last few decades, cold formed steel as a structural or a non-structural component has increasingly been used in light-gauge construction because of its high strength-to-weight ratio, which results in cost-efficient construction. Because of its advantages, CFS is used for chord studs, field studs, tracks, joists and shear wall framing. Shear wall panels are the primary lateral-load resisting components in structural systems and they sufficiently contribute to the overall structural integrity of the buildings. In particular, wood sheathed cold-formed steel framed shear walls are capable of resisting vertical push down and uplift loads and mainly lateral in-plane and out-of-plane loads, such as extreme wind loading and earthquakes.

¹ PhD Candidate, University of Massachusetts, Amherst, <fderveni@umass.edu>

² Assistant Professor, University of Massachusetts, Amherst, <sgerasimidis@umass.edu>

³ Assistant Professor, University of Massachusetts, Amherst, <kdpeterman@umass.edu>

Numerous research efforts have been conducted to evaluate the response of cold-formed steel components. A numerical, analytical and experimental investigation of sheathed cold-formed steel shear walls by Vieira and Schafer (2012) concluded that both local fastener deformations and global sheathing deformations contributed to the strength of the walls under compression loads. Buonopane et al. (2015) and Bian et al. (2015) developed fastener-based computational models of wood sheathed cold-formed steel shear walls under earthquake events, using finite element software OpenSees, concluding that fastener-based models accurately captured the shear wall performance in comparison with previous experimental findings. Ngo and Schafer (2014) and Ding and Moen (2015) developed high-fidelity wood sheathed shear wall models using finite element software ABAQUS and predicting strength and failure limit states for stud-to-sheathing connections. In addition, experimental efforts by Liu et al. (2014) and Peterman et al. (2014) evaluated connection performance of wood sheathed CFS shear walls under monotonic and cyclic loading under displacement control, while Yu (2010) experimentally examined the shear strength of different aspect ratio steel sheathed CFS shear walls under monotonic and cyclic tests.

At the full-system level, a computational modeling of a 2-story CFS building was performed by Leng et al. (2013), including diagonally braced shear wall modeling simulation to capture the global robustness of the building under earthquake loading through global collapse. The numerical results were validated by system-level experimental investigation of a 2-story CFS building under seismic excitations developed by Peterman et al. (2016), testing the full response of the building with and without non-structural components subjected to both destructive and non-destructive experimental tests.

Although numerical and experimental component-based earthquake cold-formed steel studies and system-based earthquake CFS building studies are varied in the research community, little research has been conducted in order to numerically assess the structural integrity of CFS framed shear walls by using a high fidelity finite element software and to introduce an accurate model for evaluating the stability and the failure mechanisms of sheathed CFS shear walls.

This study focuses on the evaluation of the overall response of 3D wood sheathed cold-formed steel framed shear walls subjected to lateral loads. The main purpose of this work is to introduce a robust high fidelity fastener-based simulation of wood-sheathed CFS shear walls, using finite element software ABAQUS (2014) and to validate the proposed computational tool with a previous experimental study. This work begins by introducing the model and the numerical analysis and describing the methodology assumptions of the finite element modeling approach. This is followed by the experimental validation of the finite element model. The comparison between the numerical and the experimental results is next illustrated in the results and discussion section and the failure mechanisms are presented. Finally, the conclusions section is dedicated to the observations and the explanations of the most important findings of this study, identifying future work recommendations.

2. Modeling and Numerical Analysis

The current study is a numerical work that evaluates the stability of wood sheathed cold-formed steel framed shear walls under lateral loading. The configuration adopted herein is based on the work of Ngo and Schafer (2014) and Ding and Moen (2015), as illustrated at Fig. 1. In particular, the simulated shear wall is composed of CFS chord studs, a CFS field stud, CFS tracks, oriented

strand board (OSB) sheathing at the exterior side of the wall, ledger framing at the interior side of the wall, shear anchors at the bottom of the wall and hold downs for preventing uplift. The critical parameter of an OSB sheathed CFS shear wall is the CFS-to-OSB connections; these connections and how they are modeled are the focus of this work.

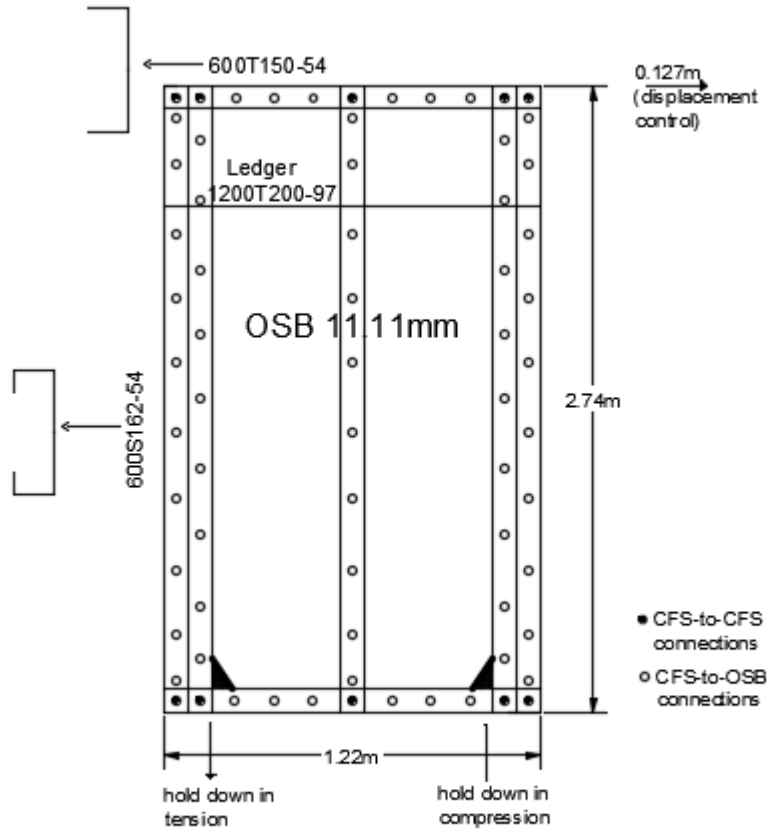


Figure 1: Geometry configuration and component details (not to scale).

2.1 Model Geometry

The CFS shear wall studied in this work has a width of 1.22m and a height of 2.74m, as depicted in Fig. 1. The frame is constructed of 600S162-54 studs and 600T150-54 tracks, while the ledger is assembled by a structural 1200T200-97 track, based on AISI-S240-15. Studs are connected to the tracks with No. 10 flathead screws, while the back-to-back chord studs are connected to each other with No. 10 flathead screws spaced every 12in. Ledger is connected to the interior side of the shear wall with No. 10 fasteners. The structural CFS frame is attached to the 11.11mm, 24/16 rated, exposure 1 by No. 8 flathead fasteners. Simpson Strong-Tie S/HDU6 hold-downs are used at the bottom of the wall attached at the interior side of the chord studs with twelve No. 14 fasteners. Seams on sheathing and geometric imperfections are ignored for simplicity in this first model. The modeling details are summarized in Table 1. Finally, the shear wall system is subjected to monotonic loading at the top of the wall. The shear wall configuration described here is adopted for comparison reasons with the experimental work following.

Table 1: Geometry details

Component	Section
Chord and field studs	600S162-54
Tracks	600T150-54
Ledger	1200T200-97
OSB sheathing	11.11mm thick
Hold-downs	S/HDU6

2.2 Finite Element Mesh Discretization

A high fidelity finite element model is introduced by simulating every component of the wall structural system by shell elements. Four-node shell elements with reduced integration points, S4R, are used from ABAQUS library in order to model both CFS members and OSB sheathing. Mesh significance is illustrated in Schafer et al. (2010) by comparing three different element types from ABAQUS library, showing the sensitivity of cold-formed steel components to element and mesh discretization. A fine mesh of a size of 6.35mm is chosen for the CFS members herein, allowing for two elements in the lips of the studs. On the other, a coarse mesh of a size of 50.8mm is chosen for OSB sheathing.

2.3 Material Properties

Cold-formed steel components are modeled as isotropic and plastic. The modulus of elasticity $E = 203\text{GPa}$ and Poisson's ratio $\nu=0.3$ are implemented in the model, while the isotropic hardening of the CFS members adopted by Moen (2009), as shown in Table 2. Plastic material is observed to avoid the unexpected large stress concentration predicted by using elastic CFS material properties and to point the regions that yielding point is reached.

Table 2: Isotropic hardening of CFS members

True Plastic Strain (mm/mm)	True Stress (MPa)
0.000	401.96
0.005	413.69
0.010	424.72
0.015	441.26
0.025	484.01
0.035	512.97
0.045	534.34
0.055	551.58
0.065	564.68
0.075	575.71
0.085	585.36
0.095	593.63
0.105	601.22

The OSB sheathing is modeled as orthotropic and elastic material, using the ENGINEERING CONSTANTS command from ABAQUS library. Based on the APA Panel Design Specification (APA 2012) the panel strength in both directions, parallel to the strength axis and perpendicular to the strength axis, is specified, as illustrated in Table 3. The panel strength is converted then to the modulus of elasticity E and shear modulus G for the sheathing material based on the

implementation of Schafer et al. (2007). Eq. 1, Eq. 2 and Eq. 3 shows the correlation of the panel strength provided to the Young's and shear modulus of the sheathing in both directions, while Table 4 depicts the orthotropic OSB material parameters used in the simulation.

Table 3: OSB Rated Panels Design Capacities

Panel bending stiffness (parallel to strength axis)	Panel bending stiffness (perpendicular to strength axis)	Panel Rigidity (through the thickness)
EI _w (kN-mm ² /mm)	EI _w (kN-mm ² /mm)	G _w t _w (kN/mm)
734.36	150.64	14.62

For modulus of elasticity in the direction parallel to the strength axis:

$$E_1 = \frac{12(EI_w)}{t_w^3} \quad (1)$$

For modulus of elasticity in the direction perpendicular to the strength axis:

$$E_2 = \frac{12(EI_w)}{t_w^3} \quad (2)$$

For shear modulus:

$$G_{12} = \frac{(G_w t_w)}{t_w} \quad (3)$$

Table 4: Converted OSB Material Parameters

Modulus of elasticity (parallel to strength axis)	Modulus of elasticity (perpendicular to strength axis)	Shear modulus (through the thickness)
E ₁ (MPa)	E ₂ (MPa)	G ₁₂ (MPa)
6422	1317	1316

Modulus of elasticity, shear modulus and Poisson's ratio need to be defined in ABAQUS in three dimensions when the material is orthotropic. In particular, Poisson's ratio equal to v=0.3 is selected for all the three dimensions. The Young's modulus E₃ in the normal to wall plane direction is assumed as E₃=E₂=1317MPa because it is not of importance in this work. Concerning the shear modulus, G₁₃=G₂₃=1316MPa, equal to G₁₂, is assumed because there is no significant out-of-plane displacement of the wall.

2.4 Fastened Connections and Hold-down Modeling

The modeling approach focuses on the connection behavior. There are two different connection types used in this study for the connections.

Firstly, the CFS-to-CFS connections are modeled by means of multi-point constraints (MPC) pinned from ABAQUS library. MPC pinned is imposed in order to constrain all the translational degrees of freedom between the two nodes but it leaves the rotations independent. CFS-to-CFS

connections appeared between the back to back chord studs, between studs and tracks and between studs and ledger. Concerning the connections between chord studs, the two back to back studs are connected in two line of connections throughout their webs. Stud-to-track connections are shown between the stud and track flanges at the top and bottom of the wall. Finally, ledger is connected to the CFS frame members at the interior of the wall in the upper location of the studs. Fig. 2b, Fig. 2c and Fig. 2d graphically show the MPC pinned connections described above.

The focal points of this study are the connections between sheathing and CFS members. Those connections represent the basic limit state in CFS shear wall behavior. For that reason, CFS-to-OSB connections are modeled as nonlinear by means of CONN3D2 connector element from ABAQUS library, as shown in Fig. 2a. The nonlinear behavior introduced to the connector elements are adopted by the experimental study by Peterman et al. (2014) by using the average of the predicted monotonic experimental behavior, as shown in Table 5. In the simulation the CARTESIAN connector element from ABAQUS library is used for the translational degrees of freedom, while the rotations are independent. Overall, the pullout-direction behavior of CFS-to-OSB connections is not observed to affect the force-displacement response of the shear wall and nonlinear connector elements are shown not to be sensitive to the gap between sheathing and studs in comparison with nonlinear springs from ABAQUS library.

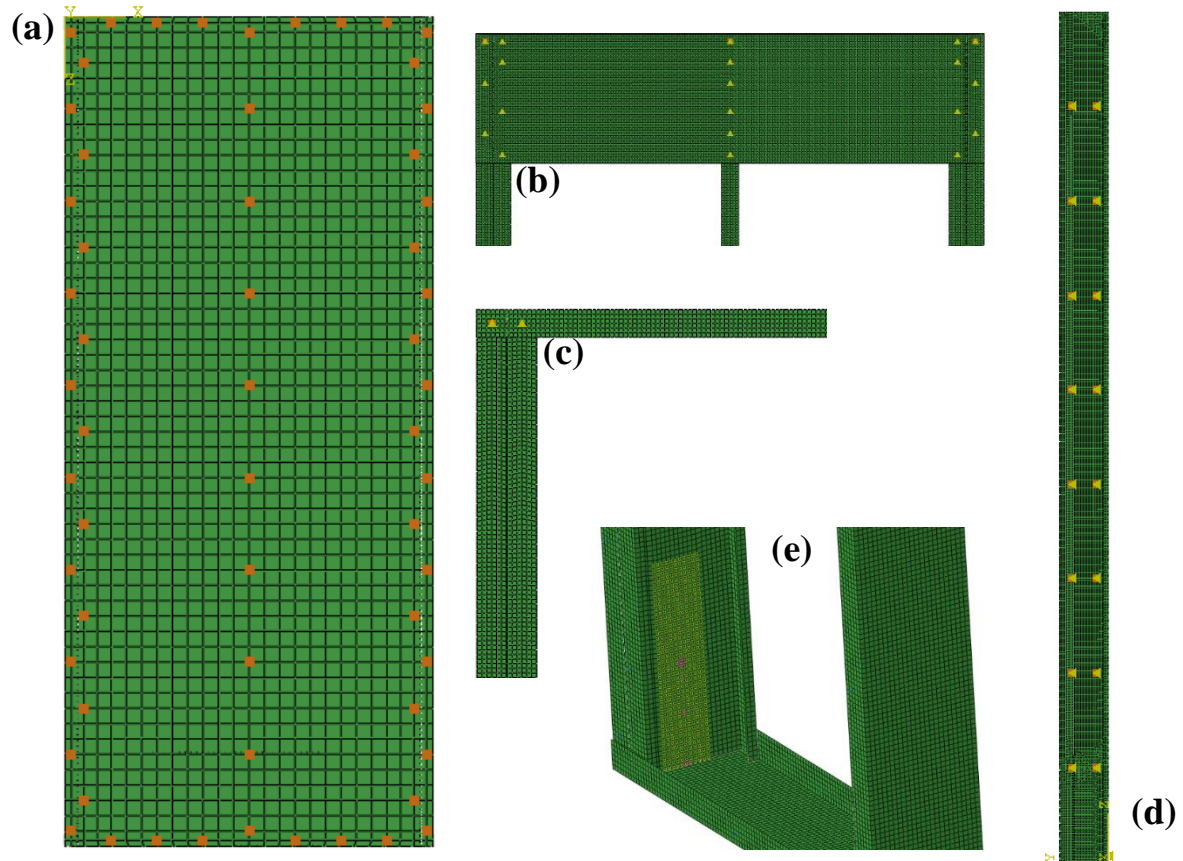


Figure 2: Connection simulation in ABAQUS. (a) CFS-to-OSB connector elements, (b) Ledger MPC pinned, (c) Stud-to-track MPC pinned, (d) Chord stud-to-chord stud MPC pinned, (e) Hold-down SPRING2.

Table 5: Monotonic Backbone Parameters of Connection Behavior

ePd ₁ (mm)	ePd ₂ (mm)	ePd ₃ (mm)	ePd ₄ (mm)	ePf ₁ (kN)	ePf ₂ (kN)	ePf ₃ (kN)	ePf ₄ (kN)
0.40	1.70	7.40	8.30	0.627	1.557	2.235	1.779
eNd ₁ (mm)	eNd ₂ (mm)	eNd ₃ (mm)	eNd ₄ (mm)	eNf ₁ (kN)	eNf ₂ (kN)	eNf ₃ (kN)	eNf ₄ (kN)
-0.40	-1.70	-7.40	-8.30	-0.627	-1.557	-2.235	-1.779

The hold-downs are modeled as a RIGID BODY at the interior side of the web of chord studs. The rigid body motion is considered at the location at which hold-downs are in contact with the web of the chord studs, as it is shown in Fig. 2e. The movement of the rigid body is controlled by a reference point (RP) which is tied at the RIGID BODY surface. This RP is connected to a fixed node at the ground by SPRING2 from ABAQUS library. SPRING2 is activated in a fixed direction preventing the uplift of the shear wall. The tension stiffness is adopted by Leng et al. (2013) as 2929kN/m, while compression stiffness is considered to be 1000 times more the tension stiffness based on the assumption that the axial force in chord studs are rigidly transferred to the foundation when the hold down is in compression. Due to the monotonic loading, one hold-down is modeled to be activated linearly in tension and the other linearly in compression.

2.5 Boundary Conditions and Contact Modeling

Shear anchors at the bottom track are modeled as pinned by restraining the horizontal and the out-of-plane movement of the wall, as depicted in Fig. 3a. At the top of the wall the out-of-plane movement of the wall is restricted by fixing the transverse direction at two lines of nodes, as shown in Fig. 3b.

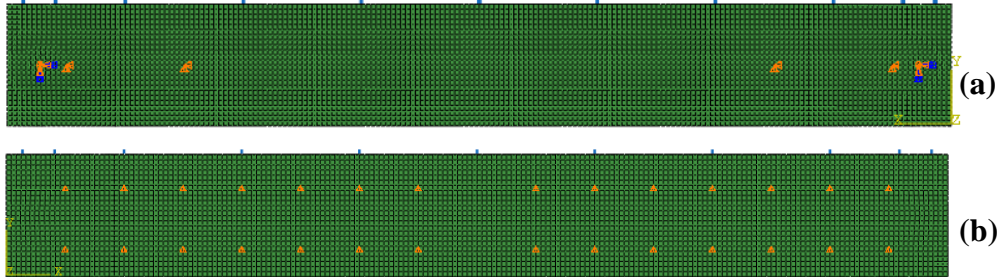


Figure 3: Boundary conditions of specimen. (a) Bottom track pinned connections at locations of shear anchors. The fixed nodes shown at the corners are used to connect the hold-downs to the ground, (b) Top track constrained out-of-plane displacement.

In the finite element analysis, many contact pairs are introduced as a surface-to-surface contact by ABAQUS library in order to simulate the interaction between members. “Hard contact” is used for the normal contact behavior assuming no penetration between CFS components and sheathing, while “hard contact” function as a normal behavior and friction coefficient of 0.2 as tangential behavior are chosen for stud-to-track interaction. The model is not sensitive to contact friction coefficients, as it is observed by the authors when friction coefficient varies from 0.2 to 0.8 in the tangential contact behavior.

2.6 Pushover Analysis

Lateral loading is introduced at the top of the wall as displacement control. A displacement of 0.127m is assigned as a boundary condition at a reference point (RP) at the center of the upper track. The reference point is tied at one edge of the track cross-section using the RIGID BODY

command from ABAQUS library. The default nonlinear solution Newton-Raphson method in ABAQUS/Standard (2014) is used and geometric nonlinearities are included in the analysis.

3. Experimental Validation of Finite Element Model

The fastener-based finite element model dimensions, materials and assumptions described above is based on the wall tested by Liu et al. (2014). Sixteen different configurations of shear walls were demonstrated, including two monotonic tests and fourteen cyclic tests. This work is focused on the lateral response of a shear wall under monotonic loading.

3.1 Test Setup and Test Specimen

The specimen was bolted at the foundation via a steel base by connecting the bottom track to the steel base with shear anchors and hold-downs. At the top of the wall, the top track was connected to a WT shape load spreader with No. 10x1" hex washer head self-drilling screws, spaced 0.076m along two lines. The steel testing frame is equipped with a 156kN hydraulic actuator with $\pm 0.127\text{m}$ and displacement control monotonic test is conducted in accordance to ASTM E564. The experimental configuration is shown in Fig. 4. Test components are previously discussed in the modeling and numerical analysis section and they are in accordance with the physical test specimen by Liu et al. (2014).



Figure 4: Oriented strand board sheathed cold-formed steel shear wall test specimen of the experimental work by Liu et al. (2014).

4. Fastener-based Modeling Findings and Results

The numerical results are compared and are shown to be validated with the experimental results by Liu et al. (2014), in terms of force-displacement response, CFS-to-OSB connections failure (frame-to-sheathing), deformation of shear wall components and ledger contribution.

4.1 Force-displacement Response

The force-displacement curve is illustrated in Fig. 5, showing that the proposed computational model accurately captures the peak base shear of the wood sheathed CFS framed shear wall by underestimating the peak load by 3.5% in comparison with the experimental work by Liu et al. (2014). Furthermore, the stiffness is reasonably captured compared to the experimental one. It needs to be mentioned herein that stiffness and strength are the subject of this work, so post-peak behavior of the wall is out of consideration.

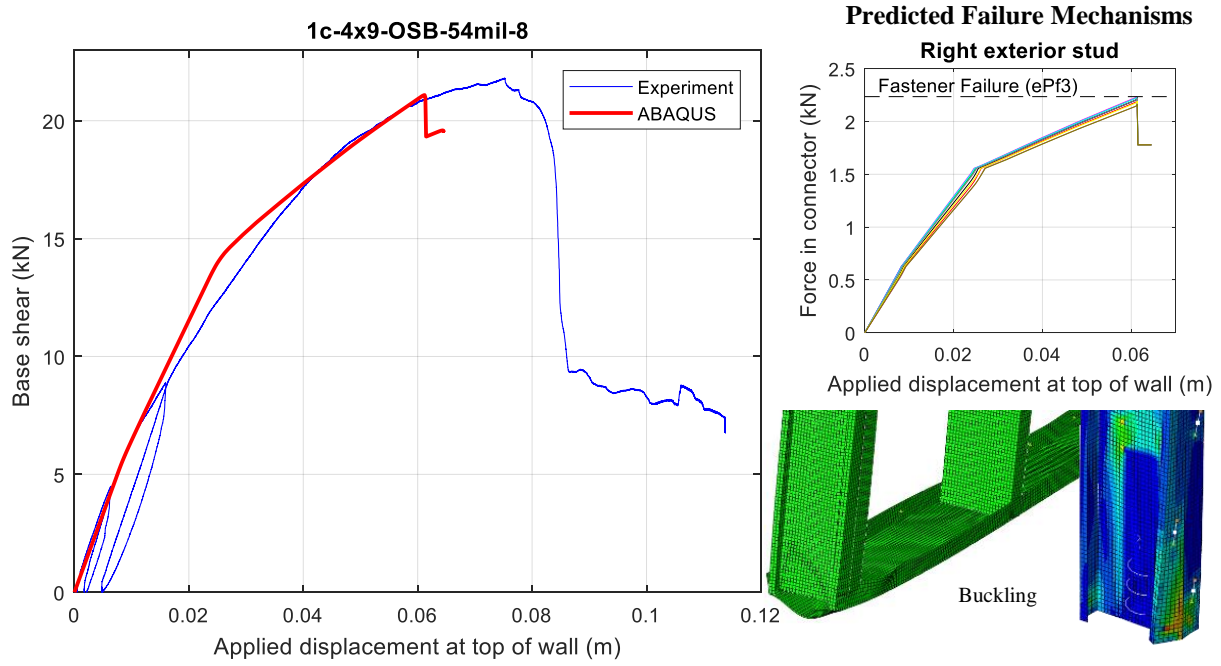


Figure 5: Computational force-displacement curve in comparison with the experimental one. Strength and stiffness of the OSB sheathed CFS shear wall is reasonably captured by the model. Failure modes are shown on the right part.

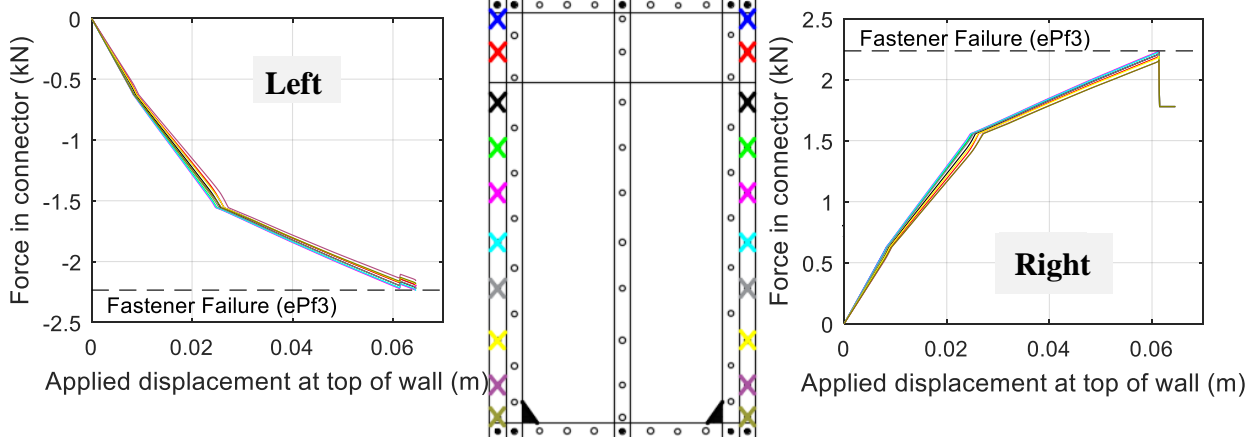
Failure modes are illustrated in Fig. 5. When the shear wall model reaches its peak load, the analysis is aborted due to OSB-to-CFS fastener failures (primary mode) and instability phenomena (secondary mode). It should be noted that while the OSB sheathing is used in order to restrain the lateral torsional buckling of the studs, flange stud buckling is observed at the bottom of the wall. Besides, the bottom track seems to fail by an abrupt change in the out of plane displacement of its flange which indicates that it buckles. In addition, high stress concentration is observed close to stud-to track connections in accordance with the experimental work.

4.2 CFS-to-OSB Connections Failure

The experimental study by Liu et al. (2014) depicts that CFS-to-OSB fasteners pull-through, edge tear out and fastener bearing are the failure mechanisms that govern the wood sheathed CFS shear wall response under lateral loading. CFS-to-OSB sheathing connection failure is observed in the numerical model in accordance to the experiment. Specifically, the chord studs-to-sheathing connections and the tracks-to-sheathing connections are predicted to fail based on the computational model. In the experimental work, bottom track-to-sheathing connection failure and bottom chord stud-to-sheathing connection failure are observed to fail, while OSB-to-sheathing connection failure is also observed around the horizontal seam location. While horizontal seam is

ignored in the computational simulation, model predicts connection failure both at the top and at the bottom of the wall. Concerning the middle part of the wall, small forces are distributed to the field stud-to-sheathing connections in both numerical and experimental work. The connections failure is shown in Fig. 6 and Fig. 7.

Exterior Studs



Interior Studs

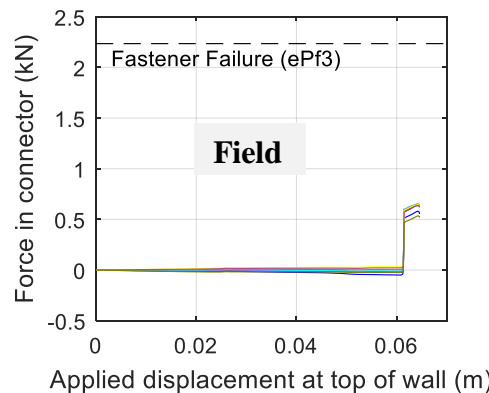
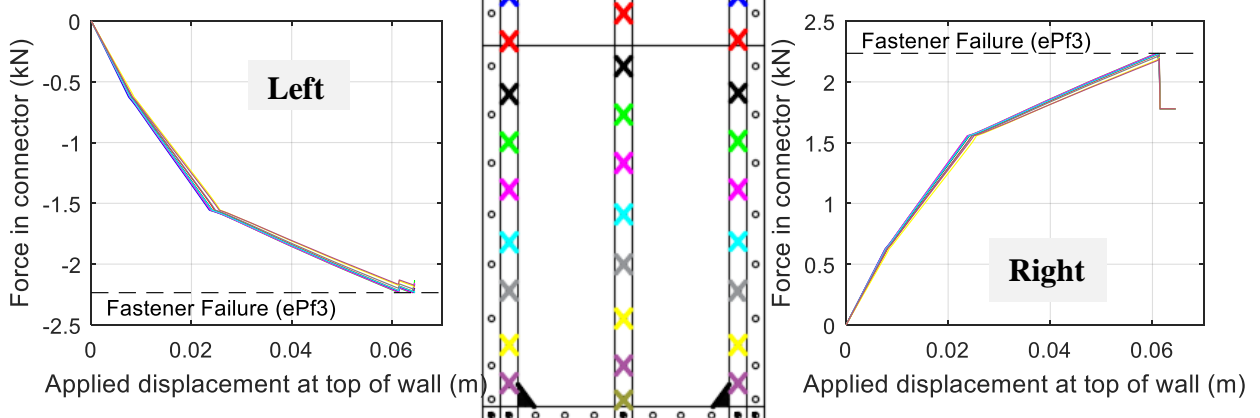


Figure 6: Fastener failure captured. Chord studs are observed to fail reaching their maximum capacities, while small forces are distributed to field stud.

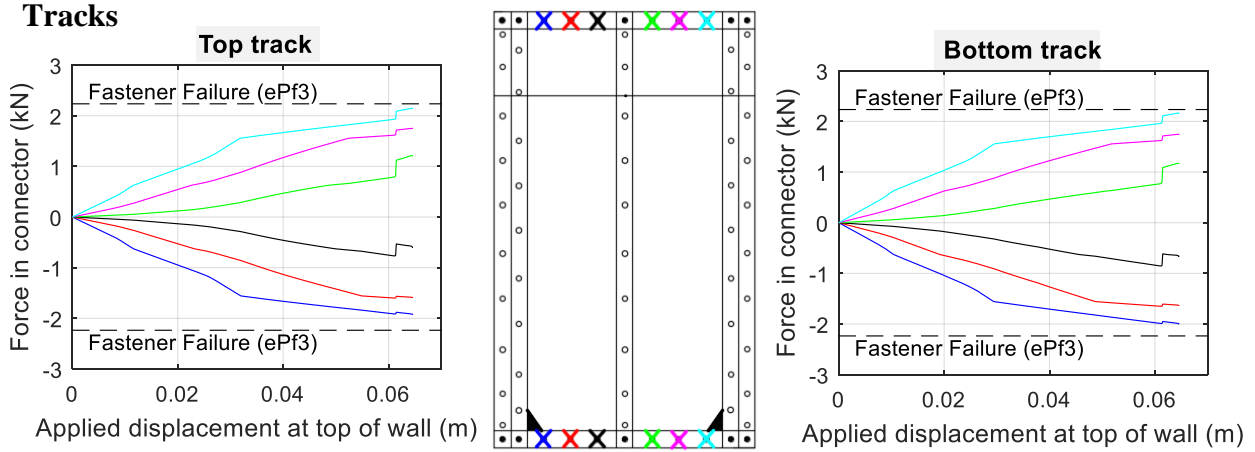


Figure 7: Fastener failure captured. Top and bottom tracks are observed to fail before fasteners reach their maximum capacities.

4.3 Deformation of Shear Wall Components and Ledger Contribution

The structural cold-formed steel frame is deformed as a parallelogram while the sheathing is mainly remaining as a rectangular shape and rotates, as illustrated in Fig. 8b. Large stress concentration is observed near to stud-to-track connection and close to the hold down regions. It is predicted that before the peak CFS-to-OSB connections failure govern, while after the peak load large deformations and instability phenomena are shown to govern.

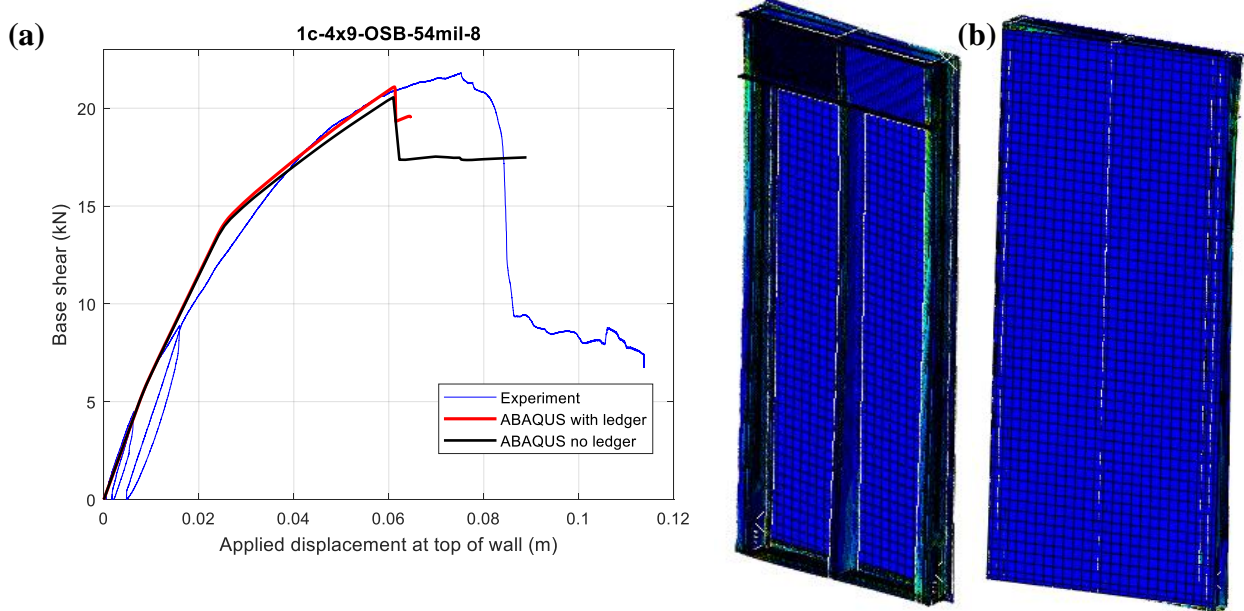


Figure 8: (a) Impact of ledger in the finite element analysis. Strength is increased when ledger is attached in accordance with the experimental work, (b) Deformed shape at the end of the analysis (scale 2).

The impact of ledger track in the OSB sheathed CFS shear wall is shown in Fig. 8a. Higher strength is predicted when ledger is attached at the interior of the CFS shear wall and this is in agreement with the experimental observations.

5. Conclusions

This work introduces an accurate high fidelity finite element model for the lateral behavior of wood sheathed cold-formed steel framed shear walls, by focusing on the nonlinear behavior of CFS-to-OSB connections. In particular, fastener-based models are shown to be capable of predicting the peak load of the wall and reasonably reproduce the force-displacement response predicted by a previous experimental study. Furthermore, the proposed model is capable of capturing the CFS-to-sheathing connection failure of wood sheathed CFS shear walls and identifying the full wall panel deformation and stress concentration in comparison with the experimental study. Finally, the ledger contribution to the strength of the wall is captured in conjunction with the experimental study.

The conclusions of the study clearly display that fastener-based models constitute a powerful tool for evaluating the behavior and the failure mechanisms of wood sheathed CFS shear walls. The implementation of this work into bigger wood sheathed CFS shear walls accounting for the use of vertical and horizontal seams at the sheathing is considered as a next step, while the extension of the model into different sheathing materials, such as steel is needed to be assessed as a future work.

It needs to be mentioned that by implementing this robust computational tool, future research can be conducted in any cold-formed steel screw-fastened connection system, such as diaphragms with a potential use of fastener-based modeling in full building simulation.

References

- Abaqus User, Manual. (2014). "Abaqus Theory Guide. Version 6.14." USA.: Dassault Systems Simulia Corp
- AISI-S240-15. (2015). North American standard for cold-formed steel structural framing-lateral provisions. *Washington, D.C.: American Iron and Steel Institute.*
- APA (2012). Panel design specification.
- ASTM E564 (2006), A. Standard practice for static load test for shear resistance of framed walls for buildings. ASTM E564. *West Conshohocken, PA: ASTM International.*
- Bian, G., Padilla-Llano, D. A., Leng, J., Buonopane, S. G., Moen, C. D., & Schafer, B. W. (2015). OpenSees modeling of cold-formed steel framed wall system. In *Proceedings of 8th International Conference on Behavior of Steel Structures in Seismic Areas.*
- Buonopane, S. G., Bian, G., Tun, T. H., & Schafer, B. W. (2015). Computationally efficient fastener-based models of cold-formed steel shear walls with wood sheathing. *Journal of Constructional Steel Research, 110*, 137-148.
- Ding, C. (2015). Monotonic and Cyclic Simulation of Screw-Fastened Connections for Cold-Formed Steel Framing (*Master thesis, Virginia Tech*).
- Leng, J., Schafer, B. W., & Buonopane, S. G. (2013, April). Modeling the seismic response of cold-formed steel framed buildings: model development for the CFS-NEES building. In *Proceedings of the Annual Stability Conference-Structural Stability Research Council, St. Louis, Missouri.*
- Liu, P., Peterman, K. D., & Schafer, B. W. (2014). Impact of construction details on OSB-sheathed cold-formed steel framed shear walls. *Journal of Constructional Steel Research, 101*, 114-123.
- Moen, C. D. (2009). Direct strength design of cold-formed steel members with perforations. (*Doctoral dissertation, John's Hopkins University*).
- Ngo, H. H. (2014). Numerical and experimental studies of wood sheathed cold-formed steel framed shear walls (*Master thesis, John' Hopkins University*).
- Peterman, K. D., Nakata, N., & Schafer, B. W. (2014). Hysteretic characterization of cold-formed steel stud-to-sheathing connections. *Journal of Constructional Steel Research, 101*, 254-264.

- Peterman, K. D., Stehman, M. J., Madsen, R. L., Buonopane, S. G., Nakata, N., & Schafer, B. W. (2016). Experimental seismic response of a full-scale cold-formed steel-framed building. I: System-level response. *Journal of Structural Engineering*, 142(12), 04016127.
- Schafer, B. W., Sangree, R., and Guan, Y. (2007). "Experiments on rotational restraint of sheathing." *Report for American Iron and Steel Institute-Committee on Framing Standards. Baltimore, Maryland*.
- Schafer, B. W., Li, Z., & Moen, C. D. (2010). Computational modeling of cold-formed steel. *Thin-Walled Structures*, 48(10-11), 752-762.
- Vieira Jr, L. C. M., & Schafer, B. W. (2012). Behavior and design of sheathed cold-formed steel stud walls under compression. *Journal of Structural Engineering*, 139(5), 772-786.
- Yu, C. (2010). Shear resistance of cold-formed steel framed shear walls with 0.686 mm, 0.762 mm, and 0.838 mm steel sheet sheathing. *Engineering Structures*, 32(6), 1522-1529.